Inorganic Chemistry
Article

Inorg. Chem. **2009**, *48*, 8227–8232 **8227**
DOI: 10.1021/ic900860c

Reinvestigation of the Uranium(3.5+) Rare-Earth Oxysulfides "$(UO)_2LnS_3$" (Ln = Yb, Y)

Geng Bang Jin,[†] Eun Sang Choi,[‡] and James A. Ibers*[,†]

[†]*Department of Chemistry, Northwestern University, 2145 Sheridan Road, Evanston, Illinois 60208-3113, and* [‡]*Department of Physics and National High Magnetic Field Laboratory, Florida State University, Tallahassee, Florida 32310*

Received May 5, 2009

Dark-red square plates of the previously reported compounds "$(UO)_2LnS_3$" (Ln = Yb, Y) have been synthesized by solid-state reactions of UOS and YbS or Y_2S_3 with Sb_2S_3 as a flux at 1273 K. The structure of these isotypic compounds was reinvestigated by single-crystal X-ray diffraction methods and an inductively coupled plasma experiment. The actual formula of "$(UO)_2LnS_3$" (Ln = Yb, Y) is $(U_{0.5}Ln_{0.5}O)_2LnS_3$, that is, $ULn_2O_2S_3$, which can be charge-balanced with U^{4+} and Ln^{3+}. The layered structure comprises $(U/Ln)O_4S_4$ square antiprisms alternating with LnS_6 octahedra. U and Ln1 atoms disorder on the eight-coordinate metal position, but Ln2 atoms occupy the six-coordinate metal position exclusively. $UYb_2O_2S_3$ is a modified Curie−Weiss paramagnet between 293 and 32 K, below which part of the paramagnetic moments go through a possible ferromagnetic transition. The band gaps of $ULn_2O_2S_3$ (Ln = Yb, Y) are around 2 eV.

Introduction

Layered ternary metal oxychalcogenides have been extensively studied because of their electronic and magnetic properties.[1] Because of the differences in the oxophilicity and chalcophilicity of the metals, oxides and chalcogenides often form individual layers with distinct electronic properties. A combination of these layers results in interesting physical properties. For example, the LnCuOQ compounds (Ln = rare-earth metal; Q = S, Se, Te), consisting of alternating charge-carrying Cu/Q layers and insulating Ln/O layers, are promising transparent p-type conductors.[2−5]

Compared to other layered metal oxychalcogenides, those containing U have been much less explored. The diffuse nature of 5f electrons of U can lead to diverse electronic and magnetic properties. For example, the UOQ compounds (Q = S, Se) are semiconductors and antiferromagnets that display considerable magnetic anisotropy.[6−9] However, uranium oxychalcogenides are very difficult to synthesize because of the high stability of uranium oxides. The compounds denoted as $(UO)_2LnS_3$ (Ln = Gd−Lu, Y)[10,11] and $(UOS)_4LuS$[12] are the only reported layered uranium oxychalcogenides besides UOQ (Q = S, Se, Te).[8,13−15]

The structures described as $(UO)_2ErS_3$[11] and $(UOS)_4LuS$[12] are closely related. The U atoms are surrounded by a combination of either eight or nine S and O atoms, and the Ln atoms are surrounded by six S atoms to form distinct UOS and LnS layers. In the crystal structure of $(UO)_2ErS_3$, there is only one independent U position and there are no S−S bonds. Charge balance then leads to the formal oxidation state of 3.5+ for U. Similarly, the formal oxidation states

*To whom correspondence should be addressed. E-mail: ibers@chem.northwestern.edu.

(1) Clarke, S. J.; Adamson, P.; Herkelrath, S. J. C.; Rutt, O. J.; Parker, D. R.; Pitcher, M. J.; Smura, C. F. *Inorg. Chem.* **2008**, *47*, 8473–8486.
(2) Inoue, S.-i.; Ueda, K.; Hosono, H.; Hamada, N. *Phys. Rev. B: Condens. Matter Mater. Phys.* **2001**, *64*, 245211–245215.
(3) Ohta, H.; Nomura, K.; Hiramatsu, H.; Ueda, K.; Kamiya, T.; Hirano, M.; Hosono, H. *Solid-State Electron.* **2003**, *47*, 2261–2267.
(4) Ueda, K.; Hosono, H.; Hamada, N. *J. Phys.: Condens. Matter* **2004**, *16*, 5179–5186.
(5) Ueda, K.; Hiramatsu, H.; Hirano, M.; Kamiya, T.; Hosono, H. *Thin Solid Films* **2006**, *496*, 8–15.
(6) Ballestracci, R.; Bertaut, E. F.; Pauthenet, R. *J. Phys. Chem. Solids* **1963**, *24*, 487–491.
(7) Murasik, A.; Suski, W.; Troc, R.; Leciejewicz, J. *Phys. Status Solidi* **1968**, *30*, 61–66.
(8) Kaczorowski, D.; Pöttgen, R.; Gajek, Z.; Zygmunt, A.; Jeitschko, W. *J. Phys. Chem. Solids* **1993**, *54*, 723–731.
(9) Sato, N.; Masuda, H.; Wakeshima, M.; Yamada, K.; Fujino, T. *J. Alloys Compd.* **1998**, *265*, 115–120.
(10) Guittard, M.; Vovan, T.; Julien-Pouzol, M.; Jaulmes, S.; Laruelle, P.; Flahaut, J. *Z. Anorg. Allg. Chem.* **1986**, *540/541*, 59–66.
(11) Jaulmes, S.; Julien-Pouzoi, M.; Guittard, M.; Vovan, T.; Laruelle, P.; Flahaut, J. *Acta Crystallogr., Sect. C: Cryst. Struct. Commun.* **1986**, *42*, 1109–1111.
(12) Jaulmes, S.; Julien-Pouzol, M.; Dugué, J.; Laurelle, P.; Vovan, T.; Guittard, M. *Acta Crystallogr., Sect. C: Cryst. Struct. Commun.* **1990**, *46*, 1205–1207.
(13) Ellert, G. V.; Kuz'micheva, G. M.; Eliseev, A. A.; Slovyanskikh, V. K.; Morozov, S. P. *Russ. J. Inorg. Chem.* (*Transl. Zh. Neorg. Khim.*) **1974**, *19*, 1548–1551.
(14) Trzebiatowski, W.; Niemiec, J.; Sepichowska, A. *Bull. Acad. Polym. Sci., Ser. Sci. Chim.* **1961**, *9*, 373–377.
(15) Haneveld, A. J. K.; Jellinek, F. *J. Inorg. Nucl. Chem.* **1964**, *26*, 1127–1128.

Published on Web 08/07/2009

of U in $(UOS)_4LuS$ are 3.5+ and 4.0+. Because of the unusual oxidation state of 3.5+ for U, we have resynthesized $(UO)_2LnS_3$ (Ln = Yb, Y) and reinvestigated their structures. Here we show that the compounds are actually $ULn_2O_2S_3$ (Ln = Yb, Y), in which charge balance is achieved with U^{4+} and Ln^{3+}. We also report optical and magnetic properties of these compounds.

Experimental Section

Syntheses. UO_2 (Strem Chemicals, 99.8%), YbS (ESPI, 99.9%), ε-Yb_2S_3 (Alfa-Aesar, 99.9%), Y_2S_3 (Alfa-Aesar, 99.9%), S (Alfa-Aesar, 99.99%), and Sb (Aldrich, 99.5%) were used as received. Sb_2S_3 was prepared from the direct reaction of the elements in a sealed fused-silica tube at 1123 K. UOS was prepared by a solid−gas reaction among UO_2, S, and C at 1213 K.[16] The purities of YbS, ε-Yb_2S_3, Y_2S_3, UOS, and Sb_2S_3 were confirmed by powder X-ray diffraction measurements. Although the original syntheses[10] were carried out at 1770−2173 K, we developed a lower-temperature synthetic route. Each reaction mixture of $ULn_2O_2S_3$ (Ln = Yb, Y) was thoroughly ground and placed in a fused-silica ampule, and then the ampule was flame-sealed under vacuum. It was first heated at 1273 K for 6 days. The resultant powder was ground with 0.100 g of Sb_2S_3 flux, the mixture was again placed in an ampule, and the ampule was then vacuum sealed. The reaction mixture was reheated to 1273 K in 40 h, kept at 1273 K for 8 days, cooled to 773 K for 8 days, and then cooled to 298 K in 8 h. The $ULn_2O_2S_3$ compounds are stable in air.

For $UYb_2O_2S_3$, the starting materials were UOS (0.147 g, 0.515 mmol) and YbS (0.053 g, 0.258 mmol). The reaction product included dark-red square plates of $UYb_2O_2S_3$ and yellow needles of ε-Yb_2S_3.[17] Also in the tube were unreacted black UOS powder and black Sb_2S_3 crystals. The majority of the $UYb_2O_2S_3$ crystals were found in the form of clumps, with ε-Yb_2S_3 needle clusters growing on the top and UOS powder growing on the bottom. The yield of $UYb_2O_2S_3$ was about 20% based on Yb.

$UY_2O_2S_3$ was synthesized from a mixture of UOS (0.161 g, 0.563 mmol) and Y_2S_3 (0.039 g, 0.140 mmol). The reaction product comprised long needles of $UY_4O_3S_5$[18] and dark-red square plates of $UY_2O_2S_3$. The yields of $UY_4O_3S_5$ and $UY_2O_2S_3$ were about 10% and 5%, respectively, based on Y. Unreacted black UOS powder, orange Y_2S_3 crystals, and black Sb_2S_3 crystals were also present.

Analyses. Several dark-red plates of $ULn_2O_2S_3$ (Ln = Yb, Y) were examined with an energy-dispersive X-ray (EDX)-equipped Hitachi S-3400 scanning electron microscope. EDX analysis showed the presence of U, Ln, and S but no evidence of Sb. O could not be detected because its emission line is below the lower limit of the instrument.

An inductively coupled plasma (ICP) measurement to quantify the U:Yb ratio was conducted on a sample of about 0.5 mg of single crystals of $UYb_2O_2S_3$. The dark-red plates were carefully selected and cleaned before being dissolved in 0.72 mL of a 68−70% HNO_3 solution. The solution was diluted to 10 mL and analyzed on a Varian VISTA-MPX instrument. Seven U and Yb standard solutions were used. The ratio U:Yb was determined to be 0.59(1).

Powder X-ray Diffraction Measurements. Powder X-ray diffraction patterns were collected with a Rigaku Geigerflex powder X-ray diffractometer with the use of Cu Kα radiation (λ = 1.5418 Å).

Crystal-Structure Determinations. Single-crystal X-ray diffraction data for $UYb_2O_2S_3$ and $UY_2O_2S_3$ were collected with the use of graphite-monochromatized Mo Kα radiation (λ = 0.710 73 Å) at 100 K on a Bruker Smart-1000 CCD diffractometer.[19] The crystal-to-detector distance was 5.023 cm. Crystal decay was monitored by recollecting 50 initial frames at the end of the data collection. Data were collected by a scan of 0.3° in ω in groups of 606 frames at φ settings of 0°, 90°, 180°, and 270°. The exposure times for $UYb_2O_2S_3$ and $UY_2O_2S_3$ were 40 and 50 s frame^{-1}, respectively. The collection of the intensity data was carried out with the program *SMART*.[19] Cell refinement and data reduction were carried out with the use of the program *APEX2*.[20] A Leitz microscope equipped with a calibrated traveling micrometer eyepiece was employed to measure accurately the dimensions of each data crystal. Face-indexed absorption corrections were performed numerically with the use of the program *XPREP*.[21] Then the program *SADABS*[19] was employed to make incident beam and decay corrections.

The *SHELXL* suite of programs was used for all calculations.[21] Beginning with the model for "$(UOS)_2ErS$", the isotropic refinement of "$(UOS)_2YbS$" proceeded smoothly to an R_1 index of 0.030. An unusual feature was that the isotropic displacement sphere for U was larger than that for Yb. (This is also true for the earlier structure determination of "$(UOS)_2ErS$".) However, this same model did not refine for $(UOS)_2YS$. The structure was solved again with the program *SHELXS*. It became clear that a successful model could only be found if the scattering density at the U position were reduced significantly. An unrestricted anisotropic model in which U and Y atoms were disordered at the U site refined successfully and led to U:Y = 0.506(6):1 (Table 1). The restricted refinement (U:Y = 0.5:1) gave the same result. The unrestricted and restricted refinements for the Yb compound are also shown in Table 1. Whereas the unrestricted refinement is slightly better, we do not consider it to be significantly so.

In all of these refinements, the displacement ellipsoids of atom S2, which is at the origin of the cell, remained positive-definite but were highly prolate. This is also true in the original structure determination of "$(UO)_2ErS_3$".[11] It may be that there is some disorder in the position of atom S2; there is no evidence in any of these structure determinations to support a lower-symmetry space group.

The program *STRUCTURE TIDY*[22] was used to standardize the positional parameters. Additional experimental details are given in Table 2 and the Supporting Information.

Magnetic Susceptibility Measurements. As noted above, $UYb_2O_2S_3$ crystals grew together with ε-Yb_2S_3[17] and UOS. Large clusters of $U_2YbO_2S_3$ crystals were crushed, and small clusters comprising 7.8 mg of $UYb_2O_2S_3$ crystals were carefully collected and then ground. The X-ray diffraction pattern of the resultant powder confirmed that it was $UYb_2O_2S_3$ contaminated by a small amount of ε-Yb_2S_3. Neither UOS nor Sb_2S_3 was detected.

The powder sample was loaded into a polycarbonate capsule holder, which was then placed in a Quantum Design MPMS instrument. Direct-current susceptibility measurements were made from 2 to 300 K under zero-field-cooled (ZFC) and field-cooled (FC) conditions. The contribution of the diamagnetic background of the sample holder was removed using the experimental values from a separate run on an empty capsule. The temperature-independent background term

(16) Larroque, R. C.; Beauvy, M. *J. Less-Common Met.* **1986**, *121*, 487–496.
(17) Sleight, A. W.; Prewitt, C. T. *Inorg. Chem.* **1968**, *7*, 2282–2288.
(18) Jin, G. B.; Choi, E. S.; Wells, D. M.; Ibers, J. A. *J. Solid State Chem.* **2009**, *182*, 1861–1866.
(19) *SMART*, version 5.054, Data Collection Software for the SMART System; Bruker Analytical X-ray Instruments, Inc.: Madison, WI, 2003.
(20) *APEX2*, version 2008.6-1, and *SAINT*, version 7.34a, Data Collection and Processing Software; Bruker Analytical X-ray Instruments, Inc.: Madison, WI, 2006.
(21) Sheldrick, G. M. *Acta Crystallogr., Sect. A: Found. Crystallogr.* **2008**, *64*, 112–122.
(22) Gelato, L. M.; Parthé, E. *J. Appl. Crystallogr.* **1987**, *20*, 139–143.

Table 1. Least-Squares Refinements for $ULn_2O_2S_3$

compound	$R(F)^a$	$R_w(F^2)^b$	U:Yb
$UYb_2O_2S_3$	0.0256	0.076	0.5:1 (restricted)
$UYb_2O_2S_3$	0.0238	0.0662	0.83(4):1 (unrestricted)[c]
$UY_2O_2S_3$	0.0162	0.0508	0.5:1 (restricted)
$UY_2O_2S_3$	0.0163	0.0507	0.506(6):1 (unrestricted)

[a] $R(F) = \sum||F_o| - |F_c||/\sum|F_o|$ for $F_o^2 > 2\sigma(F_o^2)$. [b] $R_w(F_o^2) = \{\sum[w(F_o^2 - F_c^2)^2]/\sum wF_o^4\}^{1/2}$. $w^{-1} = \sigma^2(F_o^2) + (0.0321F_o^2)^2$ for $UYb_2O_2S_3$, $w^{-1} = \sigma^2(F_o^2) + (0.02F_o^2)^2$ for $UY_2O_2S_3$. [c] The ratio found from the ICP measurement is 0.59(1):1.

Table 2. Crystal Data and Structure Refinements for $ULn_2O_2S_3$[a]

	$UYb_2O_2S_3$	$UY_2O_2S_3$
fw	712.29	544.03
a (Å)	3.7762(9)	3.8077(9)
c (Å)	20.691(5)	20.889(5)
V (Å^3)	295.0(1)	302.9(1)
ρ_c (g cm^{-3})	8.018	5.966
μ (cm^{-1})	597.61	465.95

[a] For both structures, $Z = 2$, space group = $I4/mmm$, $T = 100(2)$ K, and $\lambda = 0.71073$ Å. Values of $R(F)$ and $R_w(F_o^2)$ are given in Table 1.

(χ_0) was obtained either by extrapolating the χ vs $1/T$ curve to zero at high temperatures or by using the modified Curie−Weiss fitting at low temperatures.

A separate measurement was carried out on a sample of pure ε-Yb_2S_3 to ascertain its contribution, if any, to the magnetic measurements on the $UYb_2O_2S_3$ sample.

Single-Crystal Optical Measurements. Several red square plates of $UYb_2O_2S_3$ and $UY_2O_2S_3$ were selected and placed under light mineral oil on a glass slide. Optical absorption data were collected for each compound from 380 nm (3.27 eV) to 900 nm (1.38 eV) at 293 K with a Hitachi U6000 microscopic FT spectrophotometer. The absorbances of oil and glass were subtracted as a background.

Results

Syntheses. $UYb_2O_2S_3$ and $UY_2O_2S_3$ were originally prepared at high temperatures (> 1773 K) through solid-state reactions between UOS and LnS or Ln_2S_3.[10,11] In the present study, efforts were made to lower the reaction temperature through the use of various fluxes, including alkali-metal halides, alkali-metal chalcogenides, and Sb_2S_3. No reactions were detected below 1123 K. Between 1123 and 1273 K, alkali-metal halides and chalcogenides were observed to etch the carbon-coated fused-silica tubes and react with the rare-earth sulfides to form ternary compounds. For example, the reaction of UOS and Yb_2S_3 with KCl flux at 1223 K produced $K_3Yb_7S_{12}$, which is isostructural to $Rb_3Yb_7Se_{12}$.[23] However, Sb_2S_3 was found to be inert throughout this entire temperature range. Upon heating of UOS and YbS with Sb_2S_3 at 1273 K for 3 weeks, small crystals of $UYb_2O_2S_3$ were successfully synthesized in about 20% yield. However, the crystals were coated with UOS and ε-Yb_2S_3. Complete separation of $UYb_2O_2S_3$ from these contaminants was not possible.

Two different products were formed from the reaction of UOS and Y_2S_3 with Sb_2S_3 as a flux. One was the desired product $UY_2O_2S_3$, which was obtained in about 5% yield. The other, which was obtained in about 10% yield, was the new compound $UY_4O_3S_5$.[18] Most of the $UY_2O_2S_3$ crystals were mixed with UOS or Y_2S_3. Attempts to collect enough clean crystals for ICP and magnetic measurements failed.

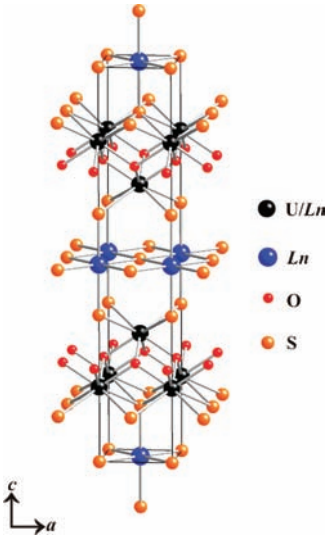

Figure 1. Two-dimensional-layered structure of $ULn_2O_2S_3$ (Ln = Yb, Y).

Numerous variations in the starting materials and stoichiometries did not improve the yields of $UYb_2O_2S_3$ or $UY_2O_2S_3$ crystals.

Structures. The structure of the isostructural compounds $UYb_2O_2S_3$ and $UY_2O_2S_3$ is shown in Figure 1. It is constructed from alternating layers of double (U/Ln)-O_4S_4 layers and single edge-sharing LnS_6 octahedral layers. The U and Ln(1) atoms, which disorder on a site of symmetry 4*mm*, are connected to four O and four S atoms in a square antiprism. The Ln(2) atoms, located on a site of symmetry 4/*mmm*, are connected to six S atoms. Within the double $(U/Ln)O_4S_4$ layers, each U/LnO_4S_4 square antiprism shares one O and two S atoms with four identical neighbors in the *ab* plane to form a single layer and further connects to four other units from the adjacent single layer by sharing two O atoms.

The structure of $ULn_2O_2S_3$ (Ln = Yb, Y) and that characterized as "$(UOS)_4LuS$"[12] are related to that of UOS,[13] as shown in Figure 2. The U atoms in UOS are surrounded by four O and five S atoms in a mono-capped square antiprism. The structure of $ULn_2O_2S_3$ (Ln = Yb, Y) can be obtained by removing all of the capping U−S bonds in the UOS structure and inserting LnS_6 octahedral layers. The structure of $(UOS)_4LuS$ can be obtained by removing half of the capping U−S bonds in the UOS structure and inserting LnS_6 octahedral layers. Therefore, half of the U atoms in the $(UOS)_4LuS$ structure are still bonded to four O and five S atoms and half of them are bonded to four O and four S atoms.

Selected interatomic distances for $UYb_2O_2S_3$ and $UY_2O_2S_3$ are listed in Table 3. The U/Ln(1) disorder does not allow detailed comparisons to be made. However, the Ln(2)−S distances clearly show the effect of the lanthanide contraction. The Yb(2)−S distances of 2.631(5) and 2.6702(6) Å are consistent with those of 2.660−2.788 Å in τ-Yb_2S_3,[24] and the Y−S distances of 2.676(2) and

(23) Kim, S.-J.; Park, S.-J.; Yun, H.; Do, J. *Inorg. Chem.* **1996**, *35*, 5283–5289.

(24) Schleid, T.; Lissner, F. *J. Alloys Compd.* **1992**, *189*, 69–74.

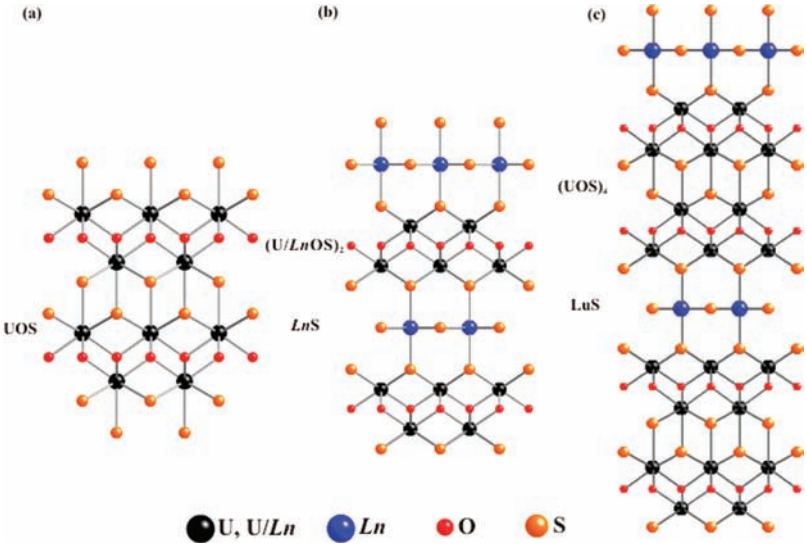

Figure 2. Views of the structures of (a) UOS, (b) $ULn_2O_2S_3$ (Ln = Yb, Y), and (c) $(UOS)_4LuS$ down the *b* axis.

Table 3. Selected Interatomic Distances (Å) for $ULn_2O_2S_3$[a,b]

	$UYb_2O_2S_3$	$UY_2O_2S_3$
U(1)/Ln(1)−O(1) × 4	2.28(2)	2.29(1)
U(1)/Ln(1)−S(1) × 4	2.96(2)	2.98(1)
Ln(2)−S(1) × 2	2.631(5)	2.676(2)
Ln(2)−S(2) × 4	2.6702(6)	2.6925(6)

[a] U(1)/Ln(1)−O and U(1)/Ln(1)−S interatomic distances are truncated to two decimal places because of the U/Ln(1) disorder. The difference between the effective ionic radii of U^{4+} and Yb^{3+} is 0.02 Å and that between U^{4+} and Y^{3+} is 0.01 Å.[39] [b] Restricted refinement.

2.6925(6) Å are in the range of those of 2.626(3)−2.819(3) Å for δ-Y_2S_3.[25]

Although bond-valence sums[26] are strictly empirical, they are often thought to provide an indication of formal oxidation states for various cations in solid-state compounds. In the present instance, the sums are as follows: for $UYb_2O_2S_3$, U(1) = 3.90, Yb(1) = 2.76, and Yb(2) = 3.25; for $UY_2O_2S_3$, U(1) = 3.76, Y(1) = 2.93, and Y(2) = 3.44.

Magnetic Susceptibility of $UYb_2O_2S_3$. Figure 3 shows the temperature dependence of the ZFC susceptibility χ and $1/\chi$ for $UYb_2O_2S_3$ at 0.1 T applied field. At both high temperatures ($100 < T < 300$ K) and low temperatures ($1.8 < T < 8$ K), the susceptibility of $UYb_2O_2S_3$ shows a modified Curie−Weiss temperature dependence ($\sim 1/T$). In the intermediate temperature range, the $1/T$ dependence starts to show deviation from the high-temperature side and a sudden increase of χ is observed below 32 K.

Before doing further analysis, we examined contributions from the possible magnetic impurities ε-Yb_2S_3 (detected from powder X-ray diffraction measurements) and UOS (not so detected). Both ε-Yb_2S_3[27] and UOS[28] are known to show a paramagnetic-to-antiferromagnetic phase transition at 7 and 55 K respectively. The dotted line of Figure 3 is $\chi(T)$ of $UYb_2O_2S_3$ after subtraction

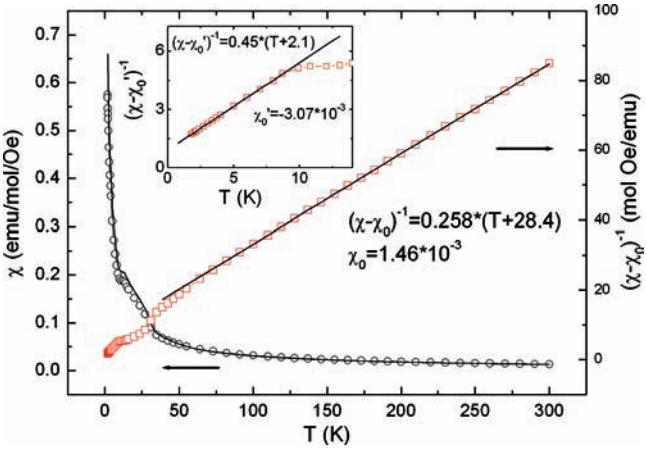

Figure 3. ZFC magnetic susceptibility χ vs T for $UYb_2O_2S_3$ under $H = 0.1$ T. The line indicates a modified Curie−Weiss fitting for χ^{-1} for $100 < T < 300$ K. The inset shows the inverse susceptibility at low temperatures with a linear fitting below 8 K. The line in the χ plot represents a hypothetical susceptibility of $UYb_2S_2O_3$ without ε-Yb_2S_3 and UOS impurities.

from the original data of contributions of 10 wt % ε-Yb_2S_3[29] and 5 wt % UOS.[28] Even though these quantities of impurities are overestimated, the two $\chi(T)$ curves are practically identical. This suggests that the $1/T$ dependence is an inherent property of $UYb_2O_2S_3$.

Nevertheless, the presence of two different magnetic ions (U^{4+} and Yb^{3+}) in $UYb_2O_2S_3$ makes it difficult to separate their contributions to the magnetic moment. For instance, a full contribution of each of the free ions (3.6 μ_B from U^{4+} and 4.9 μ_B from Yb^{3+})[30] gives $\langle\mu\rangle = [\mu(U^{4+})^2 + 2\mu(Yb^{3+})^2]^{1/2} = 7.3$ μ_B/fu, which is much larger than the observed value [5.6(2) μ_B/fu]. In fact, the values of the effective moments in rare-earth and actinide compounds are often smaller than those for the free ion because of the crystalline electric field (CEF) effect. Usually 5f electrons

(25) Schleid, T. *Eur. J. Solid State Inorg. Chem.* **1992**, *29*, 1015–1028.
(26) Brese, N. E.; O'Keeffe, M. *Acta Crystallogr., Sect. B: Struct. Sci.* **1991**, *47*, 192–197.
(27) Gruber, J. B.; Shaviv, R.; Westrum, E. F., Jr.; Burriel, R.; Beaudry, B. J.; Palmer, P. E. *J. Chem. Phys.* **1993**, *98*, 1458–1463.
(28) Amoretti, G.; Blaise, A.; Bonnet, M.; Caciuffo, R.; Erdös, P.; Nöel, H.; Santini, P. *J. Magn. Magn. Mater.* **1995**, *139*, 339–346.
(29) χ vs T of ε-Yb_2S_3 measured here shows a paramagnetic-to-antiferromagnetic transition at 5 K.
(30) Kittel, C. *Introduction to Solid State Physics*, 7th ed.; Wiley: New York, 1996.

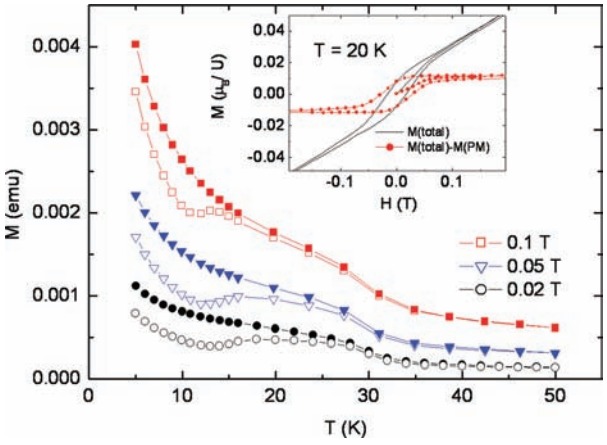

Figure 4. χ vs T for $UYb_2O_2S_3$ at different fields: ZFC (open symbols); FC (filled symbols). Inset: magnetization data taken at 20 K.

in actinides are more subject to the CEF because they tend to be less localized than the 4f electrons in rare earths. When the CEF lifts the degeneracy of the ground state of a Hund multiplet, the spin population at higher CEF levels will be decreased at finite temperatures, resulting in a reduced effective moment. The Curie-type susceptibility ($\chi \sim 1/T$) can be observed even under the CEF effect. When the temperature is much smaller than the CEF splitting, the effective moment will be reduced. When it is much larger, the free-ion value will apply.

In $UYb_2O_2S_3$, the CEF will play different roles for U^{4+} and Yb^{3+} because U^{4+} ($5f^2$, $^4H_3$) is a non-Kramers ion with a less symmetric CEF environment and Yb^{3+} ($4f^{13}$, $^2F_{7/2}$) is a Kramers ion under a rather symmetric (octahedral YbS_6) CEF field. The observed $1/T$ dependence of χ at low temperatures should be mostly from the Kramers doublet of Yb^{3+}, with the excited CEF level larger than the thermal energy. If we exploit the $1/T$ dependence by assuming a weak temperature dependence of χ of U^{4+} at low temperatures, then the effective moment of Yb^{3+} is about 3.0 μ_B. If we use this value for the $\chi \sim 1/T$ dependence at high temperatures, we obtain 3.7 μ_B for the effective moment of U^{4+}, which is very close to the free-ion value. However, we note that this is valid only with several conditions being satisfied: (1) χ of U^{4+} is weakly temperature-dependent from nonmagnetic CEF singlets at low temperatures; (2) the Yb^{3+} ground-state doublet is the only accessible energy level up to 300 K; (3) U^{4+} CEF splitting is smaller than ~100 K. Experiments involving other physical measurements would be needed to clarify the issues.

Now we turn our attention to the intermediate temperature range. The anomaly around 32 K likely arises from a ferromagnetic transition, as suggested by differences between ZFC and FC susceptibilities (Figure 4). The broad maximum of ZFC susceptibility between 13 and 20 K can be attributed to randomly oriented ferromagnetic domains. The magnetization data measured at 20 K (Figure 4 inset), which show the hysteresis and saturation of magnetization after subtraction of the paramagnetic background as estimated from the high-field region, are also typical of ferromagnetism. However, the saturation moment of 0.01 μ_B/U (or equivalently 0.005 μ_B/Yb) is much lower by 2 orders of magnitude than those of typical ferromagnetic U compounds. Very low saturation moments in actinide compounds are not unprecedented, but they have been mostly found in U−d metal intermetallics.[31] The models proposed for those compounds are not applicable to the present rare-earth compounds. Another possible cause for the anomaly around 32 K is the presence of ferromagnetic impurities that were below the level that could be detected by X-ray diffraction measurements. Impurity phases that could conceivably be present include ferromagnetic US (T_c = 180 K),[32] ferromagnetic U_3S_5(T_c = 29 K),[33] and the antiferromagnetic phases UOS (T_N = 55 K),[28] US_3 (T_N = 50 K),[34] UO_2 (T_N = 50 K),[35] Yb_2O_3 (T_N = 2.4 K),[36] and Yb_2S_2O (T_N = 2.65 K),[37] and paramagnetic US_2.[38] Among these, the only possible impurity responsible for the anomaly would be U_3S_5. From the synthetic conditions, we consider U_3S_5 to be extremely unlikely.

Even with this uncertainty, it is useful to note the difference of the magnetic structure of $UYb_2O_2S_3$ from that of UOS, which is an antiferromagnet, with the U moment being aligned along the c axis in a type 1A stacking order (++−−).[6] In UOS, U atoms within each UO_4S_4 layer couple antiferromagnetically with other U atoms from adjacent layers through U−O−U interactions. These antiferromagnetic double UOS layers stack along the c axis, and this leads to long-range antiferromagnetic ordering. To obtain the structure of $UYb_2O_2S_3$, a YbS_6 octahedral layer is inserted between two double UOS layers and half of the U atoms in the UOS layers are replaced by Yb atoms. The U−U interactions between the double layers will thereby be weakened by the increased interlayer distance. Both U−U direct exchange and U−O−U superexchange within the double layer will be weakened by dilution. U−U couplings will become less important compared to possible Yb−U or Yb−Yb interactions that we speculate may give rise to this different magnetic behavior. A further understanding of the magnetic properties of this material requires measurements on a compound with the same structure but with nonmagnetic rare-earth atoms, namely, $UY_2O_2S_3$. Unfortunately, we were unable to synthesize the necessary quantity of this material.

Optical Properties. Single-crystal absorption data, collected on several samples of $UYb_2O_2S_3$ and $UY_2O_2S_3$, are reproducible. Typical spectra of $ULn_2O_2S_3$ are plotted together with that of $UY_4O_3S_5$[18] in Figure 5. The fine structures near the absorption edge that arise from U f−f transitions are very similar in all three compounds. This is not surprising because the coordination environments of the U atoms are similar. Because of these f−f transitions, we can only estimate the band gaps to be around 2 eV, consistent with the dark-red colors of these compounds.

(31) Franse, J. J. M.; de Boer, F. R.; de Chatel, P. F.; Frings, P. H.; Menovsky, A. A. *J. Appl. Phys.* **1991**, *69*, 5903–5908.
(32) Westrum, E. F., Jr.; Walters, R. R.; Flotow, H. E.; Osborne, D. W. *J. Chem. Phys.* **1968**, *48*, 155–161.
(33) Noël, H.; Prigent, J. *Phys. B + C* **1980**, *102*, 372–379.
(34) Noël, H. *J. Less-Common Met.* **1986**, *121*, 265–270.
(35) Frazer, B. C.; Shirane, G.; Cox, D. E.; Olsen, C. E. *Phys. Rev.* **1965**, *140*, A1448–A1452.
(36) Moon, R. M.; Koehler, W. C.; Child, H. R.; Raubenheimer, L. J. *Phys. Rev.* **1968**, *176*, 722–731.
(37) Gonzalez Jimenez, F.; Imbert, P. *Solid State Commun.* **1972**, *10*, 9–13.
(38) Suski, W.; Gibinski, T.; Wojakowski, A.; Czopnik, A. *Phys. Status Solidi A* **1972**, *9*, 653–658.
(39) Shannon, R. D. *Acta Crystallogr., Sect. A: Cryst. Phys. Diffr. Theor. Gen. Crystallogr.* **1976**, *32*, 751–767.

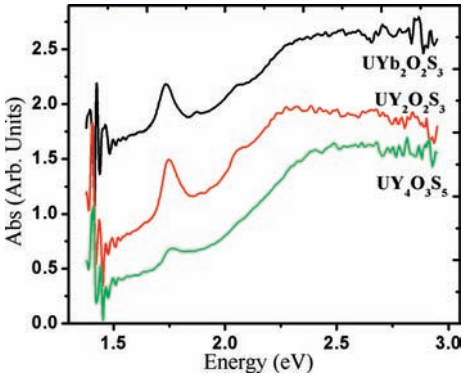

Figure 5. Single-crystal absorption spectra of $ULn_2O_2S_3$ (Ln = Yb, Y) and $UY_4O_3S_5$.

The decrease of the intensity for the transition around 1.75 eV in the order $UY_2O_2S_3$ to $UYb_2O_2S_3$ to $UY_4O_3S_5$ most probably results from the decrease of the U mass concentration.

Formal Oxidation States. One goal of the present work was to clarify the apparent oxidation state of $U^{3.5+}$ in compounds that had been characterized previously as "$(UO)_2LnS_3$" (Ln = Gd−Lu, Y),[10] on the basis of a crystal structure determination of $(UO)_2ErS_3$.[11] We were unable to solve the crystal structure of $(UO)_2YS_3$ starting with the Er model. Rather we discovered that there was U/Y disorder and that the compound is actually $UY_2O_2S_3$. Because there are no S−S interactions in the structure, charge balance leads to the formal oxidation states U^{4+} and Y^{3+}. The ionic radii of these two ions differ by only 0.01 Å, so disorder is not surprising. A similar analysis of the crystal structure of $(UO)_2YbS_3$ again reveals disorder and leads to an X-ray-derived ratio U:Yb = 0.83(3):1 (Table 1). This refinement is marginally better than one in which U:Yb is restricted to be 0.5:1, but given that the scattering powers of U (atomic number 92) and Yb (atomic number 70) are relatively close, we do not believe the two refinements differ significantly. Moreover, the U:Yb ratio of 0.59(1):1 derived from ICP measurements adds further credence to a formula of $UYb_2O_2S_3$, in which charge balance is achieved with U^{4+} and Yb^{3+}.

Crystals used for the present structure determinations were prepared from UOS and Ln_2S_3 with Sb_2S_3 as a flux at 1273 K followed by slow cooling, whereas those used in the structure determination of "$(UO)_2ErS_3$"[11] were prepared from UOS and ErS at 1770 K and rapid fusion at 2070 K followed by quenching. Are these the same materials structurally, or is it possible that the Er compound did not exhibit U/Er disorder but was indeed the $U^{3.5+}$ compound $(UO)_2ErS_3$? For the following reasons, we believe that there was U/Er disorder and that the compound was actually $UEr_2O_2S_3$: (1) The structure determinations show the same trends in displacement parameters; (2) the higher reaction conditions that generated the Er compound, both the higher temperatures and the quenching, should favor a disordered rather than an ordered structure; (3) reducing some of the U^{4+} to U^{3+} in the original preparation requires the oxidation of S^{2-} or Er^{2+} (if that is the actual oxidation state in the monosulfide). Given the great oxophilicity of U, its reduction in the presence of O^{2-} seems exceedingly unlikely.

The question then arises as to the nature of the U atoms in the compound previously described as $(UOS)_4LuS$.[12] From the structure, charge balance is achieved with equal numbers of U atoms in the formal oxidation states of $U^{3.5+}$ and U^{4+}. Given the results on the present compounds, it is reasonable to expect that undetected U/Lu disorder is the source of "$U^{3.5+}$". The effective ionic radius of U^{4+} is 0.03 Å larger than that of Lu^{3+}.[39] U and Lu atoms could disorder on the eight-coordinate metal position with an occupancy of 0.5:0.5. Alternatively, U and Lu atoms could also disorder on both eight- and nine-coordinate metal positions with an average occupancy of 0.75:0.25. In either instance, a new formula, $U_3Lu_2O_4S_5$, may be assigned in which charge balance is achieved with U^{4+} and Lu^{3+}. Specifics of the possible disorder in $(UOS)_4LuS$ must await a redetermination of its structure as well as an ICP analysis.

Acknowledgment. We thank Dr. Christos Malliakas and Prof. Mercouri G. Kanatzidis for use of their single-crystal absorption spectrometer. We also thank Adam Raw for preparing some of the starting materials and helpful discussions. This research was supported by the U.S. Department of Energy, Basic Energy Sciences, Grant ER-15522. The National High Magnetic Field Laboratory is supported by National Science Foundation through Grant NSF-DMR-0084173 and by the State of Florida.

Supporting Information Available: Crystallographic files in CIF format for $UYb_2O_2S_3$ and $UY_2O_2S_3$. This material is available free of charge via the Internet at http://pubs.acs.org.